Research Square

Preprints are preliminary reports that have not undergone peer review.
They should not be considered conclusive, used to inform clinical practice,
or referenced by the media as validated information.

Comparative Genomics of Multidrug-Resistant and Extensively Drug-Resistant Acinetobacter Baumannii Clinical Isolates from an Intensive Care Unit in Northeastern Brazil

RNDG Gondim
University Federal of Ceará (UFC)
SA Ribeiro
University Federal of Ceará (UFC)
AES Alves
University Federal of Ceará (UFC)
LFB Lino
University Federal of Ceará (UFC)
IFN Lima
University Hospital Walter Cantídio (HUWC)
LFB Nogueira
University Federal of Ceará (UFC)
Marília Maia
University Hospital Walter Cantídio (HUWC)
LMCV Magalhães
University Federal of Ceará (UFC)
LG Damasceno
University Federal of Ceará (UFC)
JQ Silva Filho
University Federal of Ceará (UFC)
DO Silva
University Federal of Ceará (UFC)
CB Mendes
Oswaldo Cruz Foundation (FIOCRUZ)
LGZ Castro
Oswaldo Cruz Foundation (FIOCRUZ)
CR Damasceno
Oswaldo Cruz Foundation (FIOCRUZ)
AMM França
Oswaldo Cruz Foundation (FIOCRUZ)

Fábio Miyajima
Oswaldo Cruz Foundation (FIOCRUZ)
Aldo Lima
University Federal of Ceará (UFC)
Alexandre Havt
University Federal of Ceará (UFC)
Marco Antonio Clementino
mclementino@ufc.br

University Federal of Ceará (UFC)

Research Article

Keywords: Acinetobacter baumannii, antimicrobial resistance, whole-genome sequencing, comparative genomics, pangenome, resistome

Posted Date: October 26th, 2026

DOI: https://doi.org/10.21203/rs.3.rs-11117075/v1

License: This work is licensed under a Creative Commons Attribution 4.0 International License.
Read Full License

Additional Declarations: No competing interests reported.

Abstract

Acinetobacter baumannii is an opportunistic pathogen linked to healthcare-associated infections and the dissemination of multidrug-resistant phenotypes in critical hospital settings. In this study, we performed a comparative genomic analysis of clinical isolates identified as *A. baumannii* by routine hospital microbiology, obtained from an intensive care unit in Northeastern Brazil and classified as susceptible (SEN), multidrug-resistant (MDR), or extensively drug-resistant (XDR). Fifteen isolates were subjected to whole-genome sequencing; after quality control, 14 genomes were included in the main comparative analyses. Genome assembly metrics, functional composition, pangenome, resistome, virulome, Pasteur MLST, core-genome phylogeny, phenotype–genotype concordance, and FastANI-based taxonomic refinement were evaluated. MDR and XDR isolates carried a higher burden of antimicrobial resistance (AMR) genes than SEN isolates. Pangenome analysis revealed a conserved core genome combined with variable accessory content, whereas the virulome was relatively conserved across phenotypic groups. Quinolone resistance-determining region (QRDR) mutations in *gyrA* and/or *parC* were detected in ciprofloxacin-resistant isolates, supporting the role of chromosomal mechanisms in fluoroquinolone resistance that may not be captured by analyses restricted to acquired resistance genes. FastANI analysis further revealed taxonomic discrepancies in two susceptible isolates, highlighting the complementary value of WGS for hospital surveillance and taxonomic refinement within the *Acinetobacter calcoaceticus–baumannii* complex. Overall, our findings indicate that antimicrobial resistance in these clinical isolates is a multifactorial phenomenon shaped by clonal diversity, accessory genome variation, AMR gene burden, chromosomal resistance mechanisms, and taxonomic complexity within the ACB complex.

INTRODUCTION

Acinetobacter baumannii is a Gram-negative opportunistic pathogen of major clinical relevance, particularly in healthcare-associated infections and intensive care units (ICUs). Its clinical importance is related to its ability to cause ventilator-associated pneumonia, bloodstream infections, urinary tract infections, wound infections, and persistent colonization in critically ill patients (1). In addition, *A. baumannii* has a remarkable ability to survive on hospital surfaces, resist desiccation, form biofilms, tolerate adverse environmental conditions, and persist under intense antimicrobial pressure, features that favor its maintenance and dissemination in critical hospital settings (2).

Antimicrobial resistance in A. baumannii represents a global public health problem. The World Health Organization has included carbapenem-resistant A. baumannii among the priority bacterial pathogens for research, development of new therapeutic alternatives, and strategies to prevent and control antimicrobial resistance (3). This scenario is particularly concerning in ICU settings, where the combination of vulnerable patients, frequent use of invasive devices, previous exposure to broad-spectrum antimicrobials, and hospital selective pressure favors the emergence and dissemination of multidrug-resistant (MDR) and extensively drug-resistant (XDR) phenotypes (4). Resistance mechanisms in A. baumannii are diverse and often act in combination. These include the production of beta-

lactamases, particularly OXA-type carbapenemases, overexpression of AmpC beta-lactamases, efflux pumps, alterations in outer membrane permeability, target modifications, chromosomal mutations, and acquisition of resistance genes through mobile genetic elements (5).

Historically, the epidemiological investigation of *A. baumannii* relied on molecular typing methods, such as pulsed-field gel electrophoresis (PFGE), to assess clonal relationships among isolates. Subsequently, multilocus sequence typing (MLST) schemes, including the Oxford and Pasteur schemes, enabled more standardized interlaboratory classification and comparison through the definition of sequence types (STs) and clonal complexes (CCs) (5,6,7). In Brazil and other Latin American countries, molecular and genomic studies have demonstrated the circulation of multiple *A. baumannii* lineages, including clonal complexes of both regional and international relevance. Among these, CC79/ST79 has frequently been associated with South America and the dissemination of multidrug-resistant clinical isolates, whereas CC15/ST15 and CC1/ST1 show broader international circulation and have also been reported in Brazilian hospitals (8,9,10). Recent genomic studies have shown that hyperendemic carbapenem-resistant *A. baumannii* clones in Brazil include CC1, CC15, CC79, and CC25, reinforcing that local epidemiology results from the coexistence of regional lineages and international clones (8,10, 11, 12).

Despite the clinical relevance of *A. baumannii*, important gaps remain regarding the genomic diversity of clinical isolates from ICUs in Northeastern Brazil. Regional studies are essential because the circulation of clones, resistance genes, mobile genetic elements, and virulence profiles may vary according to hospital, geographic, and temporal contexts. Thus, integrating phenotypic and genomic data can contribute to understanding not only which isolates are resistant, but also which genomic trajectories support the emergence, persistence, and diversification of these phenotypes. In this study, we performed a comparative genomic analysis of clinical *Acinetobacter baumannii* isolates by routine hospital microbiology, obtained from an ICU in Northeastern Brazil and classified as susceptible (SEN), multidrug-resistant (MDR), or extensively drug-resistant (XDR). We aimed to investigate the genomic determinants associated with different resistance phenotypes and to assess the complementary value of whole-genome sequencing (WGS) for hospital surveillance, molecular characterization, and taxonomic refinement within the *Acinetobacter calcoaceticus–baumannii* complex.

MATERIALS AND METHODS

Study design and ethical approval

This study included clinical isolates initially identified as *Acinetobacter baumannii* by routine hospital microbiology and recovered from the Intensive Care Unit of University Hospital Walter Cantídio (HUWC), located in Fortaleza, Ceará, Northeastern Brazil. Isolates were collected between May 2019 and April 2024. The study was approved by the local Research Ethics Committee under CAAE no. 03300218.2.0000.5054 and approval no. 3.143.258. As the study used anonymized bacterial isolates obtained as part of routine microbiological care, informed consent was waived.

The isolates were recovered from patients with suspected infection or colonization and originated from different clinical sources, including tracheal aspirates, bronchoalveolar lavage, blood cultures, urine, surgical wounds, sterile body fluids, tissue fragments, and rectal surveillance swabs. Only one isolate per patient and per species was included to avoid sample redundancy (Table 1).

Table 1
Clinical and microbiological characteristics of the isolates included in the study.

Isolate ID	Primary clinical specimen	Collection date	Collection hospital	Species identification	Resistance classification
RES014	Tracheal aspirate	05/07/2019	HUWC	*Acinetobacter baumannii*	MDR
RES047	Tracheal aspirate	07/05/2019	HUWC	*Acinetobacter baumannii*	MDR
RES052	Blood	07/16/2019	HUWC	*Acinetobacter baumannii*	XDR
RES079	Blood	08/26/2019	HUWC	*Acinetobacter baumannii*	MDR
RES087	Tracheal aspirate	09/17/2019	HUWC	*Acinetobacter baumannii*	MDR
RES131	Tracheal aspirate	02/07/2020	HUWC	*Acinetobacter baumannii*	XDR
RES158	Left thigh	10/17/2020	HUWC	*Acinetobacter baumannii*	XDR
RES168	Blood	11/17/2020	HUWC	*Acinetobacter baumannii*	MDR
RES186	Abdominal fluid	12/24/2020	HUWC	*Acinetobacter baumannii*	XDR
SEN0001	Hepatic abscess	08/16/2023	HUWC	*Acinetobacter baumannii*	SEN
SEN0006	Blood	11/18/2023	HUWC	*Acinetobacter baumannii*	SEN
SEN0010	Blood	12/26/2023	HUWC	*Acinetobacter baumannii*	SEN
SEN0015	Urine	02/14/2024	HUWC	*Acinetobacter baumannii*	SEN
SEN0017	Blood	04/11/2024	HUWC	*Acinetobacter baumannii*	SEN

Clinical source, collection date, hospital of origin, initial microbiological identification, and antimicrobial resistance classification of the 14 isolates included in the main comparative genomic analyses. SEN,

susceptible; MDR, multidrug-resistant; XDR, extensively drug-resistant; HUWC = University Hospital Walter Cantídio;

Microbiological identification and antimicrobial susceptibility testing

Initial bacterial identification and antimicrobial susceptibility testing were performed as part of routine hospital microbiology using the automated VITEK 2 Compact system (bioMérieux). Phenotypic results were classified as susceptible, intermediate, or resistant according to the interpretive criteria adopted by the laboratory, based on CLSI guidelines (13) and institutional documentation.

The following antimicrobials were evaluated: amikacin, ampicillin/sulbactam, cefepime, cefoxitin, ceftazidime, ceftriaxone, cefuroxime axetil, ciprofloxacin, colistin, gentamicin, imipenem, meropenem, piperacillin/tazobactam, and tigecycline. Based on antimicrobial susceptibility profiles, isolates were classified as susceptible (SEN), multidrug-resistant (MDR), or extensively drug-resistant (XDR), according to the international definitions proposed by Magiorakos et al. (14). MDR was defined as non-susceptibility to at least one agent in three or more antimicrobial categories, whereas XDR was defined as non-susceptibility to at least one agent in all but two or fewer antimicrobial categories.

Selection of isolates for whole-genome sequencing

Fifteen isolates initially identified as *A. baumannii* were selected for whole-genome sequencing, distributed into three phenotypic groups: five SEN, five MDR, and five XDR isolates. This selection aimed to represent different antimicrobial resistance profiles observed in the hospital routine. After sequencing and evaluation of genome assembly metrics, one XDR isolate, RES179, was excluded from the main comparative analyses due to an anomalous genome size, incompatible with the expected size for *A. baumannii*, suggesting possible mixed culture, contamination, or assembly artifact. Therefore, the main analyses were conducted with 14 genomes, comprising five SEN, five MDR, and four XDR isolates.

Genomic DNA extraction

Isolates were stored at − 80°C until DNA extraction. For bacterial recovery, frozen stocks were cultured overnight in tryptic soy broth at 37°C under agitation. On the following day, bacterial colonies were collected and subjected to genomic DNA extraction using the Wizard Genomic DNA Purification Kit (Promega), according to the manufacturer's recommendations. DNA concentration and purity were assessed by NanoDrop spectrophotometry, and isolated DNA samples were stored at − 80°C until library preparation.

Library preparation and sequencing

Genomic libraries were prepared using the Illumina DNA Prep kit according to the manufacturer's protocol. Liquid-handling steps were automated using the Dragonfly Discovery and Mosquito liquid handling systems (SPT Labtech). DNA was subjected to fragmentation, magnetic bead-based purification, indexing, amplification, and size selection using SPRI Select beads (Beckman Coulter). Library size and concentration were assessed by Qubit fluorometry. Sequencing was performed on the Illumina NextSeq 1000/2000 platform using paired-end reads.

Quality control, genome assembly, and annotation

FASTQ files generated by sequencing were subjected to a processing workflow for quality control, removal of low-quality sequences, and de novo bacterial genome assembly. Initial steps included read quality assessment, trimming/QC, and assembly into contigs by institutional bacterial WGS workflow at Fiocruz, Ceará. The resulting contigs were assessed using QUAST, including total genome size, number of contigs, N50, and GC content (15). Initial structural and functional annotation of the genomes was performed using Prokka, which identifies coding sequences, rRNAs, tRNAs, and other bacterial genomic elements (16).

Assembly metrics were used to assess the suitability of genomes for downstream comparative analyses. Genomes with sizes incompatible with the expected range for *A. baumannii*, excessive fragmentation, or evidence suggestive of possible assembly artifacts were removed from the study.

Taxonomic refinement by Average Nucleotide Identity

As a complementary taxonomic quality-control step, assembled genomes were compared with reference genomes of *A. baumannii* and *A. nosocomialis* using Average Nucleotide Identity (ANI), calculated with FastANI (17). An approximate ANI threshold of 95% was considered as a reference for bacterial species delineation. This analysis was performed after the main comparative analyses to evaluate the consistency between routine microbiological identification and genome-based species-level classification.

Pangenome analysis

Pangenome analysis was performed from genome annotation files using Panaroo, a graph-based tool designed to construct bacterial pangenomes while reducing errors arising from genome fragmentation, spurious genes, and annotation inconsistencies (18). The resulting gene presence/absence matrix was used to evaluate shared and exclusive genes among the SEN, MDR, and XDR groups.

Detection of antimicrobial resistance genes

As a complementary analysis, AMRFinderPlus was run using the *A. baumannii* organism-specific option and the --plus parameter to investigate chromosomal mutations associated with quinolone resistance

(19, 20). Initially, acquired genes and determinants associated with antimicrobial resistance detected in the assembled genomes were considered. Identified genes were organized into a binary presence/absence matrix by isolate.

Virulome characterization

Virulence-associated genes were identified by genome screening against virulence factor databases, including the Virulence Factor Database (VFDB). Genomic sequences were compared with reference virulence genes by sequence similarity, using minimum identity and coverage thresholds to define gene presence or absence. Detected genes were subsequently organized into a binary presence/absence matrix by isolate for comparison among phenotypic groups (21, 22, 23).

MLST typing

In silico MLST typing was performed using the mlst tool version 2.33.1. Available schemes for *Acinetobacter baumannii* were evaluated, with emphasis on the Pasteur scheme as the main framework for epidemiological interpretation. The Pasteur scheme includes seven housekeeping genes: *cpn60, fusA, gltA, pyrG, recA, rplB*, and *rpoB*. The formal definition of novel STs depends on submission to and validation by curated databases, such as PubMLST/BIGSdb (6, 24).

Core-genome phylogeny

Phylogenetic reconstruction was performed by maximum likelihood using IQ-TREE version 3.1.2 (25). ModelFinder was used to select the best-fit evolutionary model according to the Bayesian information criterion (BIC) (26), and branch support was estimated using ultrafast bootstrap with 1,000 replicates (27). The alignment comprised 14 sequences and 2,389,549 nucleotide sites, of which 199,862 were parsimony-informative. The best-fit model was GTR + F+I+R3. Pairwise maximum-likelihood distances generated by IQ-TREE from the same core-genome alignment were additionally examined to assess fine-scale relatedness among isolates sharing the same Pasteur ST.

KL and OCL locus typing by Kaptive

As a supplementary analysis of surface-structure diversity, *in silico* typing of capsular polysaccharide locus (KL) and lipooligosaccharide outer core locus (OCL) was performed using Kaptive with *A. baumannii*-specific reference databases (28). The best matching locus, predicted type, assignment confidence, identity, and coverage were recorded.

Statistical analysis

Categorical variables were expressed as absolute and relative frequencies. Continuous variables were described as means or medians according to data distribution, accompanied by interquartile ranges when appropriate. Comparisons among SEN, MDR, and XDR groups were performed using Fisher's exact test for categorical variables and the Kruskal–Wallis test for continuous variables, when applicable. A p-value ≤ 0.05 was considered statistically significant. Statistical analyses and graphical visualizations

were conducted in the R/RStudio environment using packages for data manipulation, multivariate analysis, graph construction, heatmaps, Venn diagrams, and phylogenetic visualization.

RESULTS

Genome assembly quality and definition of the analytical dataset

The 14 genomes included in the analyses showed assembly metrics compatible with downstream bacterial whole-genome comparative analyses (15, 29). Genome size ranged from approximately 3.7 to 4.1 Mb, with an average GC content of around 39%. The number of contigs ranged from 47 to 161, indicating moderate heterogeneity in assembly fragmentation. The number of predicted coding sequences ranged from 3,394 to 3,822 genes per isolate, suggesting overall structural conservation among the analyzed genomes, despite specific differences in gene content. Genome size, number of contigs, and N50 values are shown in **Fig. 1**.

As a complementary taxonomic refinement analysis, the assembled genomes were compared using FastANI. Most isolates showed higher genomic similarity to *A. baumannii*, with ANI values above the approximate species-level threshold. However, two susceptible isolates, SEN0006 and SEN0017, showed higher similarity to *A. nosocomialis* than to *A. baumannii*. SEN0006 showed 98.90% ANI with *A. nosocomialis* and 92.47% ANI with *A. baumannii*, whereas SEN0017 showed 98.62% ANI with *A. nosocomialis* and 92.21% ANI with *A. baumannii*. These isolates were retained in the main analyses because they reflected the initial microbiological classification used in the hospital workflow, and the taxonomic refinement results are reported in **Supplementary Table S1**.

Phylogenomic structure and distribution of Pasteur STs

Core-genome-based phylogenomic analysis revealed clusters partially associated with antimicrobial resistance phenotypes. Some MDR and XDR isolates grouped in closely related branches, suggesting shared ancestry or partial clonal dissemination. However, phylogenetic dispersion was also observed among isolates with similar resistance phenotypes, indicating that resistance may have emerged through independent acquisition of genetic determinants in different lineages, rather than exclusively through expansion of a single resistant clone. The core-genome phylogenetic tree is shown in Fig. 2.

Maximum-likelihood phylogenetic tree inferred from the core-genome alignment of 14 isolates. The alignment contained 2,389,549 nucleotide sites, including 199,862 parsimony-informative sites. Phylogenetic reconstruction was performed using IQ-TREE v3.1.2 with ModelFinder for evolutionary model selection. The best-fit model according to the Bayesian information criterion was GTR + F+I+R3, and branch support was estimated using ultrafast bootstrap with 1,000 replicates. Tip colors indicate antimicrobial resistance phenotype: susceptible (SEN), green; multidrug-resistant (MDR), blue; and extensively drug-resistant (XDR), red.

MLST typing using the Pasteur scheme demonstrated clonal diversity among the evaluated isolates. The following sequence types were identified: ST79, ST15, ST1, ST638, ST781, ST1082, and ST1356, in addition to one XDR isolate with an undetermined ST. ST79 was the predominant sequence type, identified in four MDR isolates and one XDR isolate, suggesting its importance within the evaluated dataset. Despite sharing the ST79 assignment, the four MDR isolates were not phylogenetically homogeneous. RES014, RES047, and RES079 formed a closely related subcluster, whereas RES087 showed greater core-genome divergence and clustered more closely with the XDR ST79 isolate RES052, demonstrating that ST79 affiliation did not correspond to a single MDR clone. ST15 was detected in isolates with distinct phenotypes, including one MDR and one XDR isolate, indicating that the same clonal background may be associated with different degrees of antimicrobial resistance.

Pasteur MLST profiles of clinical isolates initially identified as *A. baumannii*, grouped by resistance phenotype. Pasteur MLST identified multiple sequence types, including ST79, ST15, ST1, ST638, ST781, ST1082, and ST1356. One XDR isolate, RES186, showed an undetermined Pasteur ST due to an ambiguous or incompletely resolved fusA locus reported as Pas_fusA(431?), and was therefore conservatively retained as ST undetermined (STND).

Among susceptible isolates, greater ST diversity was observed, including ST1356, ST638, ST1082, and ST781. This clonal heterogeneity among SEN isolates was consistent with the greater dispersion observed in analyses based on gene-content profiles. The XDR isolate RES131 was assigned to ST1, whereas RES186 showed an undetermined Pasteur ST due to incomplete or ambiguous resolution of the fusA locus, despite exact assignment of the other six loci included in the Pasteur scheme. Therefore, RES186 was conservatively retained as ST undetermined and was not interpreted as a novel ST. The distribution of Pasteur STs by isolate and resistance phenotype is shown in Fig. 3.

Pangenome structure and genes shared among resistance phenotypes

Pangenome analysis demonstrated the presence of a large set of genes shared among the three phenotypic groups, indicating substantial conservation of the core genome among the analyzed isolates. Approximately 3,949 genes were common to the SEN, MDR, and XDR groups, indicating that most of the gene content was conserved within the evaluated dataset. Despite this conservation, differences were observed in accessory gene content associated with resistance phenotypes. MDR isolates showed the highest number of exclusive genes, with 361 genes restricted to this group, followed by SEN isolates, with 252 exclusive genes, and XDR isolates, with 88 exclusive genes. The distribution of shared and phenotype-associated genes is represented in the Venn diagram shown in Fig. 4A.

Functional classification of phenotype-associated genes revealed relevant differences among groups. Among genes exclusive to the SEN group, no AMR genes were identified in the functional pangenome analysis, whereas genes related to DNA regulation and repair accounted for approximately 37% of this set. In MDR isolates, genes related to DNA regulation/repair were also well represented, accounting for approximately 19.6% of exclusive genes, in addition to virulence-associated genes, which represented

approximately 9.8% of this repertoire. In XDR isolates, a higher relative proportion of genes associated with antimicrobial resistance was observed, representing approximately 18% of exclusive genes, together with mobilome-related genes, which accounted for approximately 17.9%. The functional distribution of phenotype-associated genes is shown in Fig. 4B.

Principal component analysis based on the gene presence/absence matrix revealed partial clustering patterns among isolates. MDR isolates formed a more compact cluster, suggesting greater similarity in accessory gene content. In contrast, XDR isolates showed a more heterogeneous distribution, with some isolates positioned close to MDR isolates and others more distant (Fig. 4C).

Comparative pangenome analysis of SEN, MDR, and XDR isolates initially identified as *A. baumannii*. (A) Venn diagram showing shared and phenotype-associated genes among resistance groups. (B) Functional distribution of phenotype-associated genes, including antimicrobial resistance, metabolism, mobilome, DNA regulation/repair, and virulence-related categories. (C) Principal component analysis based on gene presence/absence profiles. Each point represents one isolate colored by resistance phenotype. (D) Distribution of phenotype-associated genes, including AMR genes, annotated genes, hypothetical proteins, and virulence-associated genes. The pangenome analysis highlights a conserved core genome combined with variable accessory gene content among resistance phenotypes.

Global functional analysis of the genomes showed a predominance of functionally annotated genes in all groups, although a substantial proportion of the coding repertoire remained classified as hypothetical proteins. The mean number of functionally annotated genes was approximately 1,954 in SEN isolates, 2,025 in MDR isolates, and 2,017 in XDR isolates. In parallel, a mean of 1,479 hypothetical proteins was observed in SEN isolates, 1,677 in MDR isolates, and 1,508 in XDR isolates. MDR isolates showed a higher mean number of hypothetical proteins compared with the SEN and XDR groups (Fig. 4D).

Resistome profile

Resistome analysis, performed as a complementary curated AMR-specific screening, revealed substantial heterogeneity in the distribution of genes associated with antimicrobial resistance. This layer should be interpreted separately from the functional pangenome classification described above: the functional pangenome analysis considered phenotype-associated accessory genes from genome annotation, whereas the resistome analysis specifically screened curated AMR determinants using AMRFinderPlus. The resistome Venn diagram showed genes detected exclusively in SEN isolates (n = 7), genes exclusive to XDR isolates (n = 3), one gene shared between SEN and XDR isolates, most shared genes occurring between MDR and XDR isolates (n = 26), and only one gene common to all three groups (Fig. 5A).

The mean AMR gene burden was higher in MDR isolates, with an average of 15.6 genes per isolate, followed by XDR isolates, with an average of 13.2 genes per isolate, and SEN isolates, with an average of 2.8 genes per isolate. The AMR gene presence/absence heatmap showed more extensive resistance gene profiles among MDR and XDR isolates, whereas SEN isolates carried fewer detected determinants

(Fig. 5B). Among determinants observed in XDR isolates, genes associated with aminoglycoside and beta-lactam resistance were notable, including aac(3)-Ia, aac(6')-Ib, and blaOXA variants, whereas MDR isolates showed a broad AMR gene repertoire, particularly involving beta-lactams, aminoglycosides, tetracyclines, and phenicols (Fig. 5C).

Comparative analysis of antimicrobial resistance genes detected among SEN, MDR, and XDR isolates initially identified as *A. baumannii*. (A) Venn diagram showing shared and phenotype-associated AMR genes. (B) Presence/absence heatmap of AMR genes identified by whole-genome sequencing-based resistome screening. Blue cells indicate gene presence and red cells indicate gene absence. Hierarchical clustering was based on AMR gene presence/absence profiles. (C) Relative distribution of AMR gene classes across resistance phenotypes, including aminoglycosides, beta-lactams, macrolides, phenicols, quinolones, rifamycins, sulfonamides, tetracyclines, and trimethoprim-associated resistance determinants.

Comparison between antimicrobial susceptibility and genomic markers

Before interpretation of complementary genomic analyses, phenotypic results obtained using the VITEK 2 Compact system were compared with genomic markers initially detected in the resistome. This analysis allowed evaluation of concordance between antimicrobial susceptibility profiles observed in routine hospital microbiology and genomic determinants identified by WGS. In the comparison matrix, SEN isolates showed a predominantly concordant profile, with phenotypic susceptibility and absence of specific markers for most evaluated antimicrobials.

Among MDR and XDR isolates, broad concordance was observed for several antimicrobials, particularly when phenotypic resistance was associated with the presence of compatible genomic markers. However, specific discordances were also identified. Ciprofloxacin initially appeared as phenotypic resistance without a corresponding acquired resistance marker in several resistant isolates, whereas some antimicrobials, such as gentamicin, showed cases of genomic marker detection without corresponding phenotypic resistance. The initial phenotype–genotype concordance matrix is shown in Fig. 6.

Heatmap comparing antimicrobial susceptibility results obtained using the VITEK 2 Compact system with acquired resistance markers detected by genome-based resistome screening. Each tile represents the comparison between one isolate and one antimicrobial agent. Concordant profiles indicate resistant/intermediate phenotypes supported by compatible genomic markers or susceptible phenotypes without specific markers. Discordant profiles include phenotype-only resistance, genotype-only markers, and antimicrobials without direct genomic mapping. Quinolone resistance-associated QRDR mutations were assessed separately using AMRFinderPlus and are reported in **Supplementary Table S2**.

As a subsequent complementary analysis, AMRFinderPlus was run using the *A. baumannii* organism-specific option, allowing the identification of point mutations associated with quinolone resistance. The *gyrA_S81L* mutation was detected in all MDR and XDR isolates included in the main analysis, whereas *parC_S84L* was identified in a subset of these isolates, including RES168, RES131, RES158, and RES186 (**Supplementary Table S2**). These findings provide genomic support for the phenotypic ciprofloxacin resistance observed in antimicrobial susceptibility testing and indicate that the apparent initial discordance largely resulted from an analysis restricted to acquired resistance genes.

Virulome profile across resistance phenotypes

Virulome analysis demonstrated high conservation of virulence-associated genes among the analyzed isolates. The Venn diagram revealed a common core of 111 virulence genes shared among SEN, MDR, and XDR isolates, indicating that a large proportion of the virulence-associated repertoire was preserved regardless of resistance phenotype (Fig. 7A). In addition, five genes were exclusive to SEN isolates and 22 genes were shared between MDR and XDR isolates, whereas no genes were exclusively restricted to either the MDR or XDR group in this analysis.

The mean number of virulence genes was slightly higher among MDR and XDR isolates than among SEN isolates, with approximately 113–114 genes per isolate in the resistant groups and approximately 99 genes per isolate in the susceptible group. Despite this numerical difference, the overall virulome profile was more conserved than the resistome, suggesting that the isolates share a common set of genes associated with colonization, persistence, and adaptation to the hospital environment. Presence/absence gene analysis identified specific variations in selected determinants. The cpaA and ata genes, associated with immune evasion and adhesion/biofilm formation, respectively, were absent in XDR isolates. In contrast, effectors associated with the type VI secretion system, including *tse1, tse2, and tse3*, were detected in XDR isolates but absent among MDR isolates. The virulome heatmap and the functional distribution of virulence categories are shown in Figs. 7B and 7C.

Comparative analysis of virulence-associated genes among susceptible (SEN), multidrug-resistant (MDR), and extensively drug-resistant (XDR) isolates initially identified as *A. baumannii*. (A) Venn diagram showing shared and phenotype-associated virulence genes. (B) Presence/absence heatmap of virulence-associated genes detected by genome-based screening. Blue cells indicate gene presence and red cells indicate gene absence. Hierarchical clustering was based on virulence gene presence/absence profiles. (C) Relative distribution of virulence functional categories across resistance phenotypes, including adhesion and biofilm formation, nutrient acquisition and metabolism, surface and immune interaction, secretion systems/effectors/toxins, and virulence regulation.

KL/OCL typing by Kaptive

To evaluate surface-structure diversity among the studied isolates, in silico typing of capsular polysaccharide locus (KL) and outer core/lipooligosaccharide locus (OCL) was performed using Kaptive. Among MDR isolates, three showed a KL22/K3 profile associated with OCL10, whereas RES087 showed

KL49/OCL10 and RES168 showed KL81/K2 associated with OCL7. Among XDR isolates, RES052 showed KL9/K9-OCL10, RES131 showed KL1/K1-OCL1, and RES158 and RES186 showed KL81/K2-OCL7 (**Supplementary Table S3**). These findings suggest additional diversity in surface structures among the evaluated clinical isolates. KL/OCL assignments for SEN0006 and SEN0017 should be interpreted with caution, as FastANI analysis indicated higher similarity of these isolates to *A. nosocomialis* than to *A. baumannii*, whereas the Kaptive reference databases used in this analysis were specific for *A. baumannii*.

DISCUSSION

This study demonstrates that clinical isolates initially identified as *Acinetobacter baumannii* from an ICU in Northeastern Brazil present antimicrobial resistance as a multifactorial phenomenon that cannot be explained solely by clonal expansion or by the absolute number of resistance genes. The integration of the analyses performed in this study revealed a scenario of genomic diversity in which different lineages may reach MDR and XDR phenotypes through distinct evolutionary trajectories. This pattern is consistent with recent genomic studies describing *A. baumannii* as a pathogen with high genomic plasticity, in which resistance, hospital adaptation, and environmental persistence result from the interaction of acquired genes, chromosomal mutations, mobile genetic elements, accessory genome variation, and clonal background (5, 12, 30). Thus, our findings reinforce that genomic surveillance of clinical isolates should go beyond the simple detection of AMR genes, incorporating population structure, pangenome composition, chromosomal resistance mechanisms, virulence factors, and taxonomic accuracy within the *Acinetobacter calcoaceticus–baumannii* complex.

Phylogenomic analysis and Pasteur MLST typing indicated that resistance phenotypes were not associated with a single clonal lineage. ST79 was predominant among MDR isolates and was also detected in one XDR isolate, a finding compatible with the relevance of CC79/ST79 in Brazil and South America (12). Importantly, the four MDR isolates assigned to ST79 did not represent a single genetically homogeneous group. Although RES014, RES047, and RES079 formed a closely related core-genome subcluster, RES087 showed substantially greater genomic divergence and was more closely related to the XDR isolate RES052 than to the other MDR ST79 isolates. Moreover, closely related isolates were observed across different resistance phenotypes, indicating that phylogenetic relatedness and MDR/XDR classification were not strictly congruent. Brazilian genomic studies have demonstrated the circulation of multiple *A. baumannii* clonal complexes, including CC79, CC15, CC1, and CC113, with CC79 frequently associated with multidrug-resistant clinical isolates and regional dissemination in South America (10, 11). The presence of ST79 in the analyzed dataset therefore reinforces the importance of South American lineages in the local epidemiology of *A. baumannii* in Fortaleza, Ceará, Brazil.

The identification of ST15 and ST1 expands this epidemiological interpretation. ST15/CC15 has been described in Brazilian and South American isolates, including MDR lineages associated with carbapenem resistance, whereas ST1/CC1 corresponds to an internationally disseminated lineage (31). The coexistence of ST79, ST15, and ST1 in the same hospital dataset suggests that the evaluated ICU does not reflect the expansion of a single clone, but rather the presence of lineages with different evolutionary

and epidemiological histories. This pattern is consistent with large-scale WGS studies showing that international clones coexist with relevant regional lineages and that Latin America presents clonal and resistance profiles distinct from those observed in other geographic regions (5). Recent global studies have shown that, although international clones dominate part of the epidemiology of carbapenem-resistant *A. baumannii*, local and regional lineages may play an important role in hospital dissemination, reinforcing the need for genomic studies in geographic areas that remain underrepresented in global surveillance datasets (5, 31).

Less frequently documented STs in this dataset, such as ST638, ST781, ST1082, and ST1356, appear less prominently in the recent literature compared with ST79, ST15, and ST1. However, their presence among susceptible isolates suggests additional clonal diversity within the sampled population. This diversity among SEN isolates may reflect lower selective pressure from specific antimicrobials, differences in the clinical origin of the isolates, or limitations related to the small sample size. These findings further support the importance of regional WGS studies, particularly in areas underrepresented in global genomic surveillance databases.

The isolate RES186 showed an undetermined Pasteur ST due to incomplete or ambiguous resolution of the fusA locus, despite exact assignment of the other six loci included in the Pasteur scheme. Complementary BLAST inspection indicated a signal compatible with fusA_431, although it was fragmented or only partially resolved. Therefore, classification as ST undetermined is more appropriate than assigning a novel ST. The formal definition of novel STs depends on submission to and validation by specific curated databases, such as PubMLST/BIGSdb (24).

Pangenome analysis revealed a large set of genes shared among groups, indicating substantial conservation of the core genome, but also demonstrated differences in accessory gene content among phenotypes. MDR isolates showed the highest number of exclusive genes, followed by SEN and XDR isolates. The lower number of exclusive genes in the XDR group suggests that the extensively resistant phenotype does not necessarily depend on a broad and distinct repertoire of exclusive genes. Instead, XDR isolates may represent lineages that acquired specific determinants, chromosomal mutations, regulatory changes, or genomic rearrangements capable of expanding the resistance spectrum without producing a large expansion of the exclusive gene set (30, 32). This interpretation is consistent with the absence of an exclusively XDR cluster in both PCA and phylogeny, suggesting that extreme resistance may emerge through independent trajectories.

The functional composition of phenotype-associated genes further supports the role of the accessory genome in hospital adaptation. The presence of mobilome-related genes among genes associated with resistant groups suggests the contribution of mobile genetic elements, plasmids, transposons, integrons, or genomic islands to the acquisition and redistribution of adaptive determinants. In *A. baumannii*, the accessory genome is recognized as a central component of genomic plasticity and may contribute to antimicrobial resistance, environmental survival, stress response, and persistence on hospital surfaces (33, 34).

The resistome showed a higher mean AMR gene burden in MDR and XDR isolates than in susceptible isolates. This trend is expected given the greater antimicrobial exposure and selection pressure in critical healthcare settings. However, in the present dataset, the XDR group did not show the highest absolute AMR gene burden despite exhibiting a broader resistance phenotype. This result suggests that the XDR phenotype does not depend solely on the quantitative accumulation of resistance genes, but may reflect the presence of specific determinants, chromosomal mutations, regulatory changes, genomic rearrangements, or combinations of resistance mechanisms. This interpretation is compatible with the multifactorial nature of resistance in *A. baumannii*, in which beta-lactamases, efflux pumps, permeability alterations, loss or modification of porins, mutations in antimicrobial targets, mobile elements, and genomic context may act in combination to broaden the resistance spectrum (5, 30, 32, 35). These findings indicate that resistome architecture does not follow a simple separation between susceptible and resistant isolates, but rather involves partial overlap of genetic determinants among phenotypes.

The detection of resistance-associated determinants among isolates classified as susceptible should be interpreted in light of the analytical layer used and the biological context. Genes such as *bla*ADC variants, *bla*OXA variants, and *tet*(39) may be present without necessarily producing phenotypic resistance to the antimicrobial tested. In *A. baumannii*, intrinsic or acquired beta-lactamases may depend on insertion sequences or promoter elements, such as ISAba1 or ISAba125, to reach expression levels sufficient to affect the resistance phenotype (36, 37). Therefore, the mere presence of genes such as *bla*ADC or *bla*OXA variants should not be interpreted in isolation as clinical resistance. Similarly, tetracycline determinants such as *tet*(39) are associated with efflux and tetracycline resistance, but their relationship with phenotype depends on genetic context, expression, and the specific antimicrobial evaluated (38,39,40). Thus, in the present study, the detection of these genes in isolates classified as susceptible should be interpreted as the presence of resistance-associated determinants, and not as direct evidence of phenotypic resistance (32, 37, 38, 41).

Comparison between the phenotypic profile obtained using VITEK and genomic resistance markers revealed biologically interpretable discordances. In the initial matrix, ciprofloxacin appeared as phenotypic resistance without a corresponding acquired resistance marker in several MDR and XDR isolates. This pattern is expected when the analysis is restricted to acquired genes, because fluoroquinolone resistance in *A. baumannii* frequently involves chromosomal mutations in quinolone resistance-determining regions, especially in *gyrA* and *parC* (42, 43). Complementary analysis with AMRFinderPlus identified *gyrA_S81L* in MDR and XDR isolates and *parC_S84L* in a subset of these isolates, providing genomic support for the phenotypic ciprofloxacin resistance observed in antimicrobial susceptibility testing. Therefore, the apparent initial discordance does not necessarily represent a failure of the genomic approach, but rather highlights the need to integrate acquired resistance genes and chromosomal mutations for accurate resistance interpretation.

The discordance observed for gentamicin may reflect the limited specificity of some aminoglycoside resistance markers when interpreted only at the class level. Determinants such as *aadA*, encoding

ANT(3")(9)-type aminoglycoside nucleotidyltransferases, are classically associated with streptomycin and spectinomycin resistance; therefore, their detection alone should not be interpreted as a reliable predictor of gentamicin resistance (44, 45). The presence of aminoglycoside resistance genes should be interpreted considering gene–drug specificity, since different aminoglycoside-modifying enzymes have distinct substrate spectra (44, 46, 47).

In contrast to the resistome, the virulome was relatively conserved across phenotypic groups. Most isolates retained a broad repertoire of genes associated with adhesion, biofilm formation, nutrient acquisition, cell surface structures, regulation, and secretion systems. This pattern suggests that the capacity for colonization, persistence, and hospital adaptation may be preserved regardless of resistance phenotype. Discrete changes, such as the absence of cpaA and ata in XDR isolates and the presence of T6SS effectors in XDR isolates, may indicate specific variations in selected virulence determinants, but not a global remodeling of the virulome (2, 48, 49). Therefore, whereas the resistome appears to more clearly differentiate MDR/XDR isolates from susceptible isolates, the virulome seems to reflect a common adaptive background shared by the evaluated clinical isolates.

Kaptive analysis added an additional layer to genomic characterization by revealing diversity in loci associated with capsular polysaccharide (KL) and outer core/lipooligosaccharide (OCL). These loci encode important bacterial surface structures and may influence biologically relevant properties in *A. baumannii*, including host interaction, immune evasion, serum resistance, biofilm formation, environmental persistence, and susceptibility to bacteriophages. In the present study, different KL/OCL profiles were observed among isolates, including KL22/K3-OCL10 in multiple MDR isolates, KL81/K2-OCL7 in RES168, RES158, and RES186, KL9/K9-OCL10 in RES052, and KL1/K1-OCL1 in RES131. This pattern suggests additional diversity in surface structures among clinical lineages, even in a small dataset, and reinforces that hospital adaptation in *A. baumannii* may involve not only resistance genes but also variation in surface components with potential impact on persistence, transmission, and host–pathogen interaction. However, these findings should be interpreted as exploratory, since KL/OCL typing was performed in silico and was not accompanied by functional assays assessing capsule expression, biofilm formation, serum resistance, or virulence (1, 28, 50).

A methodologically relevant finding was the FastANI-based taxonomic refinement. Although the isolates were initially identified as *A. baumannii* by routine hospital microbiology, SEN0006 and SEN0017 showed higher genomic similarity to *A. nosocomialis* than to *A. baumannii*. This result should be interpreted in the context of the well-recognized difficulty of discriminating closely related species within the *Acinetobacter calcoaceticus–baumannii* complex using conventional phenotypic or automated methods. The retention of these isolates in the main analyses reflects the original clinical classification used in the hospital workflow and allows transparent discussion of how WGS may reveal taxonomic discrepancies not detected in routine microbiology. Thus, this finding provides evidence of the complementary value of genomics for hospital surveillance.

Our findings contribute to understanding the genomic diversity of clinical isolates from the *A. baumannii* complex in an ICU in Northeastern Brazil. The results indicate that antimicrobial resistance in this context is supported by multiple biological layers, including clonal diversity, variable accessory gene content, AMR genes, QRDR mutations, relative conservation of the virulome, and WGS-based taxonomic refinement. Together, these findings reinforce that genomic surveillance can complement hospital microbiology by enabling the understanding not only of which isolates are resistant, but also of which genomic trajectories may sustain the emergence and persistence of these phenotypes in the hospital environment.

CONCLUSION

This study demonstrates that clinical isolates identified as *Acinetobacter baumannii* from an ICU in Northeastern Brazil exhibit relevant genomic diversity and distinct antimicrobial resistance profiles. MDR and XDR phenotypes were associated with a higher AMR gene burden, but were not explained exclusively by the absolute number of resistance determinants, suggesting additional contributions from the accessory genome, specific resistance determinants, chromosomal mutations, and independent evolutionary trajectories. The virulome was relatively conserved across groups, indicating the maintenance of repertoires associated with colonization, persistence, and hospital adaptation. The comparison between VITEK results and genomic markers revealed interpretable discordances, particularly for ciprofloxacin, which were subsequently supported by the detection of QRDR mutations in *gyrA* and/or *parC*. In addition, FastANI-based taxonomic refinement revealed discrepancies between routine microbiological identification and genome-based classification in part of the susceptible isolates. Together, these findings reinforce that WGS adds value to hospital surveillance by integrating resistance, virulence, clonal structure, pangenome composition, and taxonomic resolution within the *Acinetobacter calcoaceticus–baumannii* complex.

Declaration of generative AI and AI-assisted technologies in the manuscript preparation process

During the preparation of this work, the author(s) used ChatGTP Plus (version 5.2, OPENAI) for support language refinement, structural organization, clarity improvement, and formatting of sections of the text. The AI tool was not used to generate original scientific data, perform analysis, interpret results, or create figures or tables. All experimental design, data collection, statistical analyses, data interpretation, and scientific conclusions were development and verified exclusively by the authors. The authors reviewed and edited the output as needed and take full responsibility for the content of the published article.

Declarations

Acknowledgements

The authors gratefully acknowledge the Oswaldo Cruz Foundation (Fiocruz) for providing whole-genome sequencing (WGS) support. R.N.D.G. acknowledges the Ceará Foundation for Scientific and Technological Development Support (FUNCAP) for the postdoctoral fellowship. The authors also acknowledge the Coordination for the Improvement of Higher Education Personnel (CAPES) for financial support related to publication costs. We thank the Núcleo de Biomedicina (NUBIMED), Federal University of Ceará, for providing the infrastructure and laboratory facilities necessary for this study.

Corresponding author: Marco Clementino, mclementino@ufc.br

Author Contributions

R.N.D.G.G. conceived and designed the study, performed the genomic and bioinformatic analyses, interpreted the results, prepared the figures and tables, and wrote the original manuscript. S.A.R., A.E.S.A., L.F.B.L., L.F.B.N., M.M., L.M.C.V.M., L.G.D., J.Q.S.F., and D.O.S. contributed to the methodology, investigation, laboratory procedures, and data curation. I.F.N.L. contributed to the selection of clinical isolates and the curation of clinical and microbiological data. C.B.M., L.G.Z.C., C.R.D., A.M.M.F., and F.M. contributed to whole-genome sequencing, genomic data generation, quality control, and bioinformatic support. M.A.F.C. contributed to the study conception, genomic methodology, interpretation of the bioinformatic findings, and supervision. A.A.M.L. and A.H. provided resources, project administration, supervision, funding acquisition, and critical revision of the manuscript. All authors reviewed and approved the final version of the manuscript.

Data Availability

The datasets generated and analyzed during the current study are available from the corresponding author upon reasonable request. Supplementary data supporting the findings are included with the article and its Supplementary Information.

References

1. Harding CM, Hennon SW, Feldman MF (2018) Uncovering the mechanisms of *Acinetobacter baumannii* virulence. Nat Rev Microbiol 16(2):91–102. 10.1038/nrmicro.2017.148
2. Weidensdorfer M, Ishikawa M, Hori K, Linke D, Djahanschiri B, Iruegas R et al (2019) The *Acinetobacter* trimeric autotransporter adhesin Ata controls key virulence traits of *Acinetobacter baumannii*. Virulence 10(1):68–81. 10.1080/21505594.2018.1558693
3. World Health Organization (2024) WHO bacterial priority pathogens list, 2024: bacterial pathogens of public health importance to guide research, development and strategies to prevent and control antimicrobial resistance. World Health Organization, Geneva. Licence: CC BY-NC-SA 3.0 IGO
4. Ye B, Wu W, Zhang R, Lu W, Wei X, Ye H et al (2024) Risk factors for multidrug-resistant and extensively drug-resistant *Acinetobacter baumannii* infection of patients admitted in intensive care

unit: a systematic review and meta-analysis. J Hosp Infect 148:77–86. 10.1016/j.jhin.2024.04.004

5. Müller C, Reuter S, Wille J, Xanthopoulou K, Stefanik D, Grundmann H, Higgins PG, Seifert H (2023) A global view on carbapenem-resistant *Acinetobacter baumannii*. mBio 14:e02260–e02223. 10.1128/mbio.02260-23
6. Jolley KA, Bray JE, Maiden MCJ (2018) Open-access bacterial population genomics: BIGSdb software, the PubMLST.org website and their applications. Wellcome Open Res 3:124. 10.12688/wellcomeopenres.14826.1
7. Gaiarsa S, Batisti Biffignandi G, Esposito EP, Castelli M, Jolley KA, Brisse S et al (2019) Comparative analysis of the two *Acinetobacter baumannii* multilocus sequence typing (MLST) schemes. Front Microbiol 10:930. 10.3389/fmicb.2019.00930
8. Chagas TPG, Carvalho KR, Santos ICO, Carvalho-Assef APD, Asensi MD (2014) Characterization of carbapenem-resistant *Acinetobacter baumannii* in Brazil (2008–2011): countrywide spread of OXA-23-producing clones (CC15 and CC79). Diagn Microbiol Infect Dis 79(4):468–472. 10.1016/j.diagmicrobio.2014.03.006
9. Camargo CH, Tiba MR, Saes MR, Vasconcellos FMD, Santos LFD, Romero EC, Garcia DO (2016) Population structure analysis of carbapenem-resistant *Acinetobacter baumannii* clinical isolates from Brazil reveals predominance of clonal complexes 1, 15, and 79. Antimicrob Agents Chemother 60(4):2545–2547. 10.1128/AAC.02186-15
10. Nodari CS, Cayô R, Streling AP, Lei F, Wille J, Almeida MS et al (2020) Genomic analysis of carbapenem-resistant *Acinetobacter baumannii* isolates belonging to major endemic clones in South America. Front Microbiol 11:584603. 10.3389/fmicb.2020.584603
11. Camargo CH, Cunha MPV, Barcellos TAF, Bueno MS, Bertani AMJ, Santos CA et al (2020) Genomic and phenotypic characterisation of antimicrobial resistance in carbapenem-resistant *Acinetobacter baumannii* hyperendemic clones CC1, CC15, CC79 and CC25. Int J Antimicrob Agents 56(6):106195. 10.1016/j.ijantimicag.2020.106195
12. Leal NC, Campos TL, Rezende AM, Docena C, Mendes-Marques CL, Sá Cavalcanti FL et al (2020) Comparative genomics of *Acinetobacter baumannii* clinical strains from Brazil reveals polyclonal dissemination and selective exchange of mobile genetic elements associated with resistance genes. Front Microbiol 11:1176. 10.3389/fmicb.2020.01176
13. Clinical and Laboratory Standards Institute (2026) Performance Standards for Antimicrobial Susceptibility Testing. 36th ed. CLSI supplement M100. Wayne, PA: Clinical and Laboratory Standards Institute
14. Magiorakos AP, Srinivasan A, Carey RB, Carmeli Y, Falagas ME, Giske CG et al (2012) Multidrug-resistant, extensively drug-resistant and pandrug-resistant bacteria: an international expert proposal for interim standard definitions for acquired resistance. Clin Microbiol Infect 18(3):268–281. 10.1111/j.1469-0691.2011.03570.x
15. Gurevich A, Saveliev V, Vyahhi N, Tesler G (2013) QUAST: quality assessment tool for genome assemblies. Bioinformatics 29(8):1072–1075. 10.1093/bioinformatics/btt086

16. Seemann T (2014) Prokka: rapid prokaryotic genome annotation. Bioinformatics 30(14):2068–2069. 10.1093/bioinformatics/btu153
17. Jain C, Rodriguez-R LM, Phillippy AM, Konstantinidis KT, Aluru S (2018) High-throughput ANI analysis of 90K prokaryotic genomes reveals clear species boundaries. Nat Commun 9:5114. 10.1038/s41467-018-07641-9
18. Tonkin-Hill G, MacAlasdair N, Ruis C, Weimann A, Horesh G, Lees JA et al (2020) Producing polished prokaryotic pangenomes with the Panaroo pipeline. Genome Biol 21:180. 10.1186/s13059-020-02090-4
19. Feldgarden M, Brover V, Gonzalez-Escalona N, Frye JG, Haendiges J, Haft DH et al (2021) AMRFinderPlus and the Reference Gene Catalog facilitate examination of the genomic links among antimicrobial resistance, stress response, and virulence. Sci Rep 11:12728. 10.1038/s41598-021-91456-0
20. Feldgarden M, Brover V, Fedorov B, Haft DH, Prasad AB, Klimke W (2022) Curation of the AMRFinderPlus databases: applications, functionality and impact. Microb Genomics 8(6):mgen000832. 10.1099/mgen.0.000832
21. Camacho C, Coulouris G, Avagyan V, Ma N, Papadopoulos J, Bealer K, Madden TL (2009) BLAST+: architecture and applications. BMC Bioinformatics 10:421. 10.1186/1471-2105-10-421
22. Chen L, Zheng D, Liu B, Yang J, Jin Q (2016) — 10 years on. Nucleic Acids Res 44(D1):D694–D697. 10.1093/nar/gkv1239. VFDB 2016: hierarchical and refined dataset for big data analysis
23. Liu B, Zheng D, Zhou S, Chen L, Yang J (2022) VFDB 2022: a general classification scheme for bacterial virulence factors. Nucleic Acids Res 50(D1):D912–D917. 10.1093/nar/gkab1107
24. PubMLST (2026) Curators: allelic profiles/STs. PubMLST Curators Guide. Available from: https://pubmlst.org/. Accessed 3 July
25. Nguyen LT, Schmidt HA, von Haeseler A, Minh BQ (2015) IQ-TREE: a fast and effective stochastic algorithm for estimating maximum-likelihood phylogenies. Mol Biol Evol 32(1):268–274. 10.1093/molbev/msu300
26. Kalyaanamoorthy S, Minh BQ, Wong TKF, von Haeseler A, Jermiin LS (2017) ModelFinder: fast model selection for accurate phylogenetic estimates. Nat Methods 14(6):587–589. 10.1038/nmeth.4285
27. Hoang DT, Chernomor O, von Haeseler A, Minh BQ, Vinh LS (2018) UFBoot2: improving the ultrafast bootstrap approximation. Mol Biol Evol 35(2):518–522. 10.1093/molbev/msx281
28. Wyres KL, Cahill SM, Holt KE, Hall RM, Kenyon JJ (2020) Identification of *Acinetobacter baumannii* loci for capsular polysaccharide (KL) and lipooligosaccharide outer core (OCL) synthesis in genome assemblies using curated reference databases compatible with Kaptive. Microb Genomics 6(3):e000339. 10.1099/mgen.0.000339
29. Pearl S, Anbarasu A (2025) Genomic landscape of nosocomial *Acinetobacter baumannii*: a comprehensive analysis of the resistome, virulome, and mobilome. Sci Rep 15:18203. 10.1038/s41598-025-03246-7

30. Rodrigues DLN, Morais-Rodrigues F, Hurtado R, Santos RG, Costa DC, Barh D (2021) Pan-resistome insights into the multidrug resistance of *Acinetobacter baumannii*. Antibiotics 10(5):596. 10.3390/antibiotics10050596
31. Frenk S, Temkin E, Lurie-Weinberger MN, Keren-Paz A, Rov R, Rakovitsky N et al (2022) Large-scale WGS of carbapenem-resistant *Acinetobacter baumannii* isolates reveals patterns of dissemination of ST clades associated with antibiotic resistance. J Antimicrob Chemother 77(4):934–943. 10.1093/jac/dkac010
32. Kyriakidis I, Vasileiou E, Pana ZD, Tragiannidis A (2021) *Acinetobacter baumannii* antibiotic resistance mechanisms. Pathogens 10(3):373. 10.3390/pathogens10030373
33. Imperi F, Antunes LCS, Blom J, Villa L, Iacono M, Visca P, Carattoli A (2011) The genomics of *Acinetobacter baumannii*: insights into genome plasticity, antimicrobial resistance and pathogenicity. IUBMB Life 63(12):1068–1074. 10.1002/iub.531
34. Mangas EL, Rubio A, Álvarez-Marín R, Labrador-Herrera G, Pachón J, Pachón-Ibáñez ME (2019) Pangenome of *Acinetobacter baumannii* uncovers two groups of genomes, one of them with genes involved in CRISPR/Cas defence systems associated with the absence of plasmids and exclusive genes for biofilm formation. Microb Genomics 5(11):e000309. 10.1099/mgen.0.000309
35. Wu HJ, Wang AH, Jennings MP (2023) Drug-resistant *Acinetobacter baumannii*. Experimental Therapeutic Med 25:124. 10.3892/etm.2023.11908
36. Turton JF, Ward ME, Woodford N, Kaufmann ME, Pike R, Livermore DM, Pitt TL (2006) The role of ISAba1 in expression of OXA carbapenemase genes in *Acinetobacter baumannii*. FEMS Microbiol Lett 258(1):72–77. 10.1111/j.1574-6968.2006.00195.x
37. Lopes BS, Amyes SGB (2012) Role of ISAba1 and ISAba125 in governing the expression of *blaADC* in clinically relevant *Acinetobacter baumannii* strains resistant to cephalosporins. J Med Microbiol 61(Pt 8):1103–1108. 10.1099/jmm.0.044156-0
38. Agersø Y, Guardabassi L (2005) Identification of Tet 39, a novel class of tetracycline resistance determinant in *Acinetobacter* spp. of environmental and clinical origin. J Antimicrob Chemother 55(4):566–569. 10.1093/jac/dki051
39. Rumbo C, Gato E, López M, Ruiz de Alegría C, Fernández-Cuenca F, Martínez-Martínez L et al (2013) Contribution of efflux pumps, porins, and β-lactamases to multidrug resistance in clinical isolates of *Acinetobacter baumannii*. Antimicrob Agents Chemother 57(11):5247–5257. 10.1128/AAC.00730-13
40. Akers KS, Mende K, Yun HC, Hospenthal DR, Beckius ML, Yu X, Murray CK (2009) Tetracycline susceptibility testing and resistance genes in isolates of *Acinetobacter baumannii–Acinetobacter calcoaceticus* complex from a U.S. military hospital. Antimicrob Agents Chemother 53(6):2693–2695. 10.1128/AAC.01405-08
41. Pagano M, Martins AF, Machado ABMP, Barin J, Barth AL (2013) Carbapenem-susceptible *Acinetobacter baumannii* carrying the ISAba1 upstream *blaOXA-51-like* gene in Porto Alegre, southern Brazil. Epidemiol Infect 141(2):330–333. 10.1017/S095026881200074X

42. Zaki MES, Abou ElKheir N, Mofreh M (2018) Molecular study of quinolone resistance-determining regions of *gyrA* gene and *parC* genes in clinical isolates of *Acinetobacter baumannii* resistant to fluoroquinolones. Open Microbiol J 12:116–122. 10.2174/1874285801812010116
43. Mohammed MA, Alnour TMS, Shakurfo OM, Aburass MM (2021) Impact of target site mutations and plasmid-associated resistance genes acquisition on resistance of *Acinetobacter baumannii* to fluoroquinolones. Sci Rep 11:20136. 10.1038/s41598-021-99230-y
44. Ramirez MS, Tolmasky ME (2010) Aminoglycoside modifying enzymes. Drug Resist Updates 13(6):151–171. 10.1016/j.drup.2010.08.003
45. Kehrenberg C, Catry B, Haesebrouck F, de Kruif A, Schwarz S (2005) Novel spectinomycin/streptomycin resistance gene, *aadA14*, from *Pasteurella multocida*. *Antimicrobial Agents and Chemotherapy*. ;49(7):3046–3049. 10.1128/AAC.49.7.3046-3049.2005
46. Clark NC, Olsvik Ø, Swenson JM, Spiegel CA, Tenover FC (1999) Detection of a streptomycin/spectinomycin adenylyltransferase gene (*aadA*) in *Enterococcus faecalis*. Antimicrob Agents Chemother 43(1):157–160. 10.1128/AAC.43.1.157
47. Stern AL, van der Verren SE, Kanchugal PS, Näsvall J, Gutiérrez-de-Terán H, Selmer M (2018) Structural mechanism of AadA, a dual-specificity aminoglycoside adenylyltransferase from *Salmonella enterica*. J Biol Chem 293(29):11481–11490. 10.1074/jbc.RA118.003352
48. Li P, Tang Y, Chen Y (2023) Uncovering the secretion systems of *Acinetobacter baumannii*. Front Cell Infect Microbiol 13:1125818. 10.3389/fcimb.2023.1125818
49. Weber BS, Miyata ST, Iwashkiw JA, Mortensen BL, Skaar EP, Pukatzki S, Feldman MF (2013) Genomic and functional analysis of the type VI secretion system in *Acinetobacter*. PLoS ONE 8(1):e55142. 10.1371/journal.pone.0055142
50. Geisinger E, Isberg RR (2015) Antibiotic modulation of capsular exopolysaccharide and virulence in *Acinetobacter baumannii*. PLoS Pathog 11(2):e1004691. 10.1371/journal.ppat.1004691

Table

Table 1 is available in the Supplementary Files section.

Figures

Figure 1. Genome assembly quality metrics of clinical *Acinetobacter baumannii isolates.*

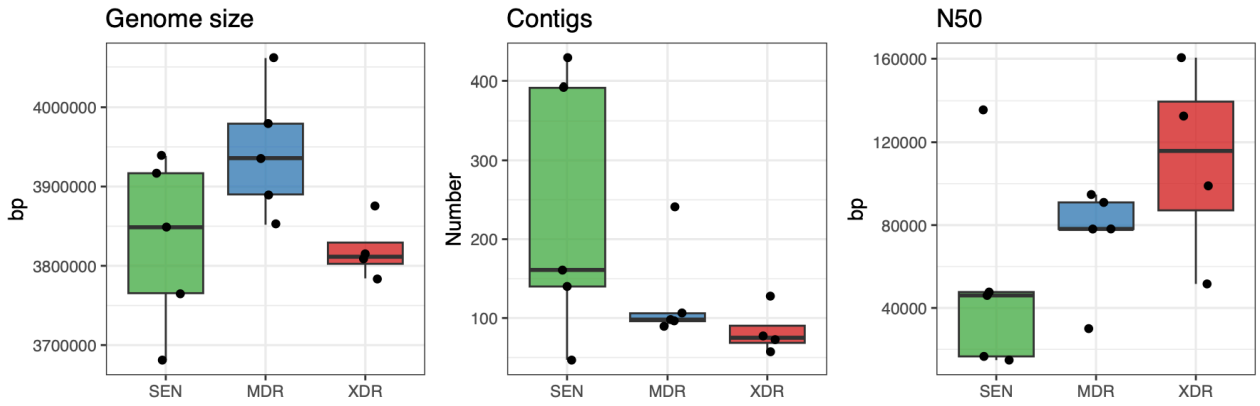

Boxplots showing genome size, number of contigs, and N50 values among susceptible (SEN), multidrug-resistant (MDR), and extensively drug-resistant (XDR) isolates initially identified as *Acinetobacter baumannii*. Each point represents one isolate. One XDR isolate was excluded from downstream analyses due to an anomalous genome size incompatible with the expected genome size of *A. baumannii*. The remaining assemblies showed genome sizes, GC content, contig numbers, and N50 values compatible with downstream comparative genomic analyses.

Figure 1

See image above for figure legend

Figure 2. Core-genome phylogeny of clinical *Acinetobacter baumannii* isolates.

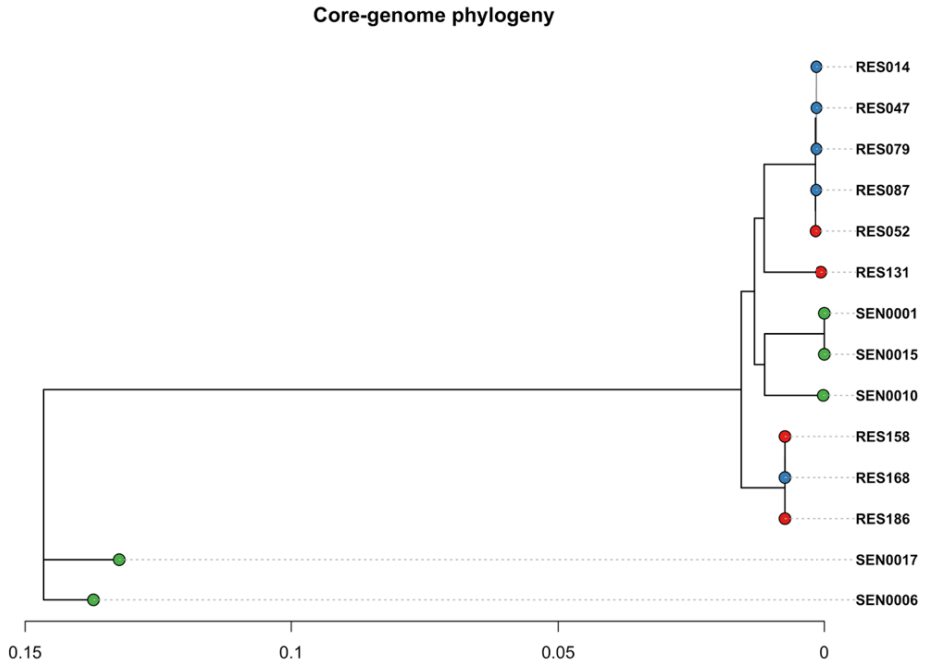

Maximum-likelihood phylogenetic tree inferred from the core-genome alignment of 14 isolates. The alignment contained 2,389,549 nucleotide sites, including 199,862 parsimony-informative sites. Phylogenetic reconstruction was performed using IQ-TREE v3.1.2 with ModelFinder for evolutionary model selection. The best-fit model according to the Bayesian information criterion was GTR+F+I+R3, and branch support was estimated using ultrafast bootstrap with 1,000 replicates. Tip colors indicate antimicrobial resistance phenotype: susceptible (SEN), green; multidrug-resistant (MDR), blue; and extensively drug-resistant (XDR), red.

Figure 2

See image above for figure legend

Figure 3. Pasteur MLST distribution among clinical *Acinetobacter baumannii* isolates.

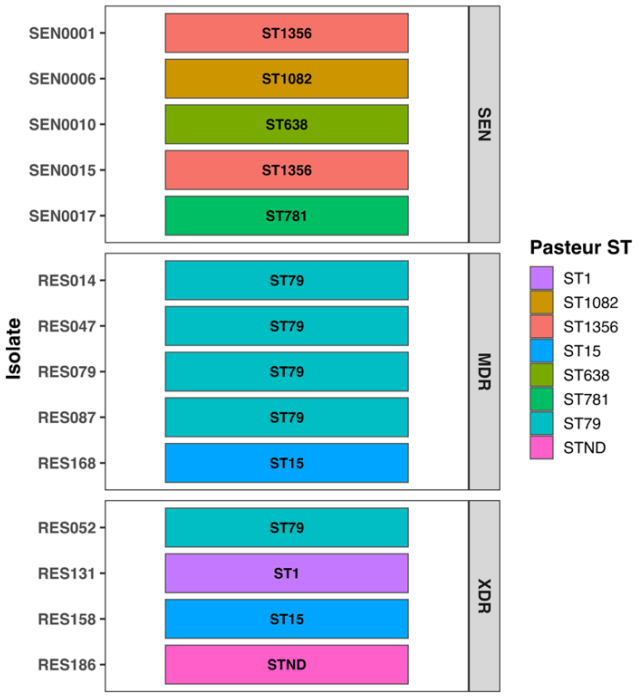

Pasteur MLST profiles of clinical isolates initially identified as *A. baumannii*, grouped by resistance phenotype. Pasteur MLST identified multiple sequence types, including ST79, ST15, ST1, ST638, ST781, ST1082, and ST1356. One XDR isolate, RES186, showed an undetermined Pasteur ST due to an ambiguous or incompletely resolved fusA locus reported as Pas_fusA(431?), and was therefore conservatively retained as ST undetermined (STND).

Figure 3

See image above for figure legend

Figure 4. Pangenome structure and accessory gene distribution according to resistance phenotype.

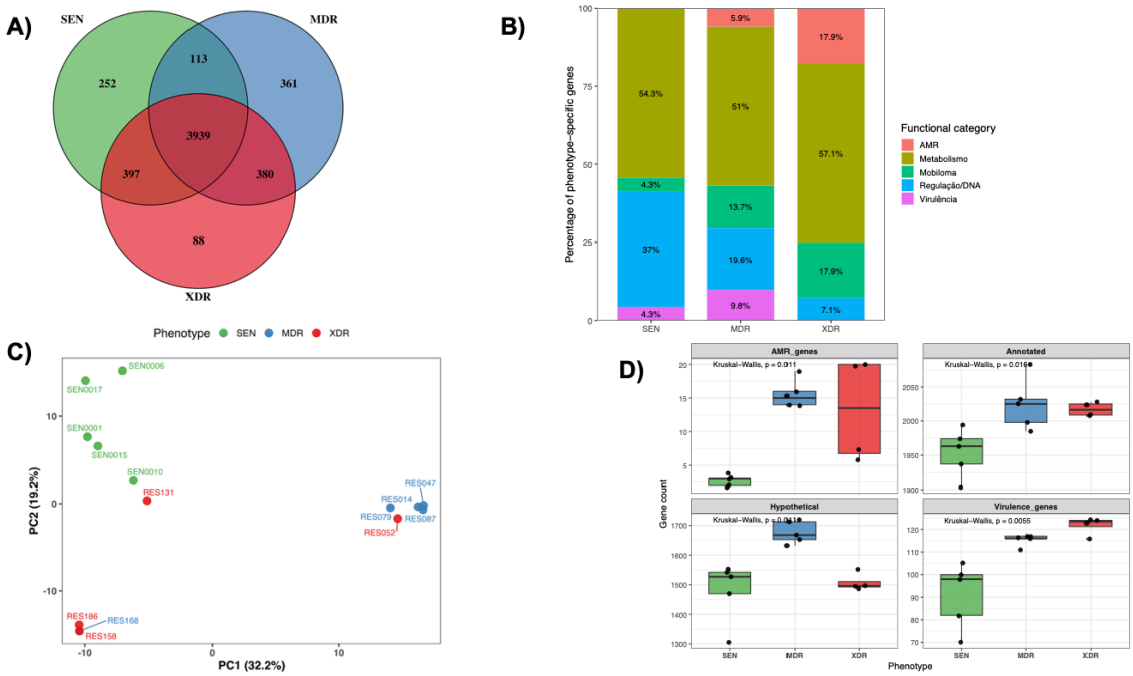

Comparative pangenome analysis of SEN, MDR, and XDR isolates initially identified as *A. baumannii*. (A) Venn diagram showing shared and phenotype-associated genes among resistance groups. (B) Functional distribution of phenotype-associated genes, including antimicrobial resistance, metabolism, mobilome, DNA regulation/repair, and virulence-related categories. (C) Principal component analysis based on gene presence/absence profiles. Each point represents one isolate colored by resistance phenotype. (D) Distribution of phenotype-associated genes, including AMR genes, annotated genes, hypothetical proteins, and virulence-associated genes. The pangenome analysis highlights a conserved core genome combined with variable accessory gene content among resistance phenotypes.

Figure 4

See image above for figure legend

Figure 5. Resistome profiles of clinical *Acinetobacter baumannii* isolates.

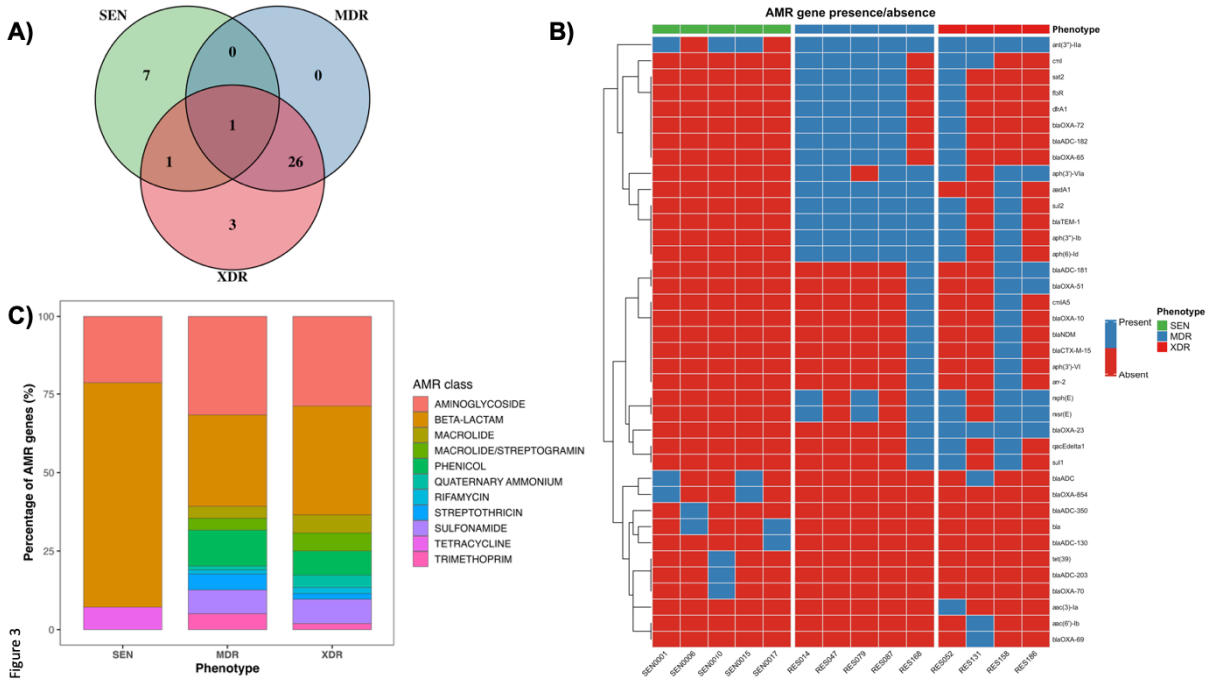

Comparative analysis of antimicrobial resistance genes detected among SEN, MDR, and XDR isolates initially identified as *A. baumannii*. (A) Venn diagram showing shared and phenotype-associated AMR genes. (B) Presence/absence heatmap of AMR genes identified by whole-genome sequencing-based resistome screening. Blue cells indicate gene presence and red cells indicate gene absence. Hierarchical clustering was based on AMR gene presence/absence profiles. (C) Relative distribution of AMR gene classes across resistance phenotypes, including aminoglycosides, beta-lactams, macrolides, phenicols, quinolones, rifamycins, sulfonamides, tetracyclines, and trimethoprim-associated resistance determinants.

Figure 5

See image above for figure legend

Figure 6. Initial phenotype–genotype comparison between VITEK antimicrobial susceptibility testing and acquired resistome markers.

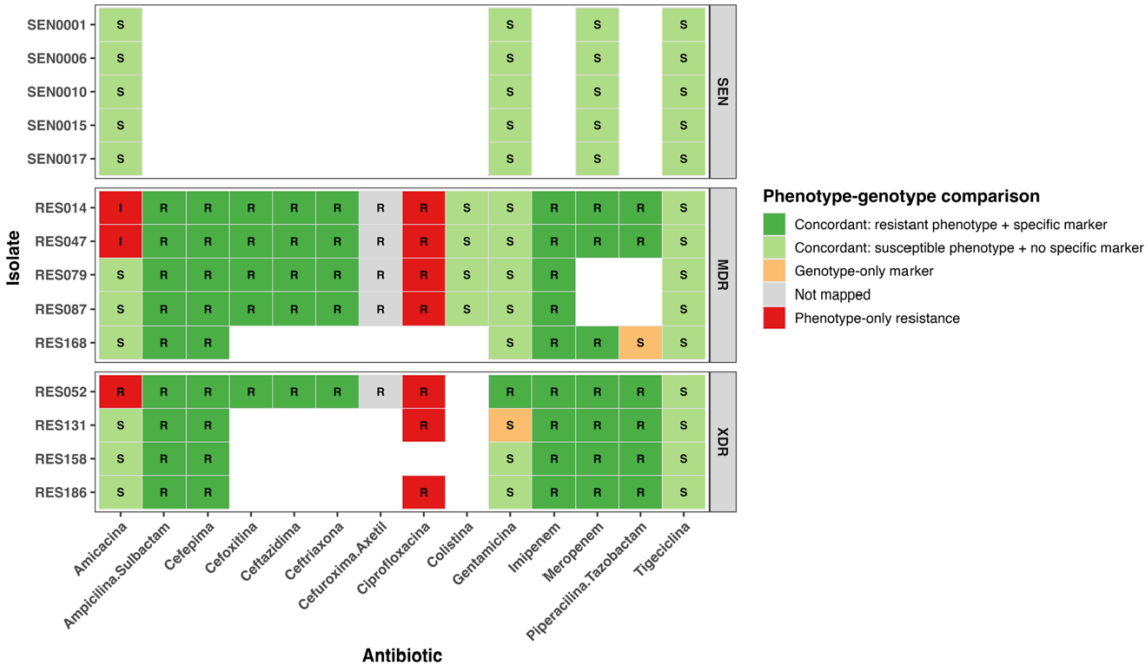

Heatmap comparing antimicrobial susceptibility results obtained using the VITEK 2 Compact system with acquired resistance markers detected by genome-based resistome screening. Each tile represents the comparison between one isolate and one antimicrobial agent. Concordant profiles indicate resistant/intermediate phenotypes supported by compatible genomic markers or susceptible phenotypes without specific markers. Discordant profiles include phenotype-only resistance, genotype-only markers, and antimicrobials without direct genomic mapping. Quinolone resistance-associated QRDR mutations were assessed separately using AMRFinderPlus and are reported in **Supplementary Table S2**.

Figure 6

See image above for figure legend

Figure 7. Virulome profiles of clinical *Acinetobacter baumannii* isolates.

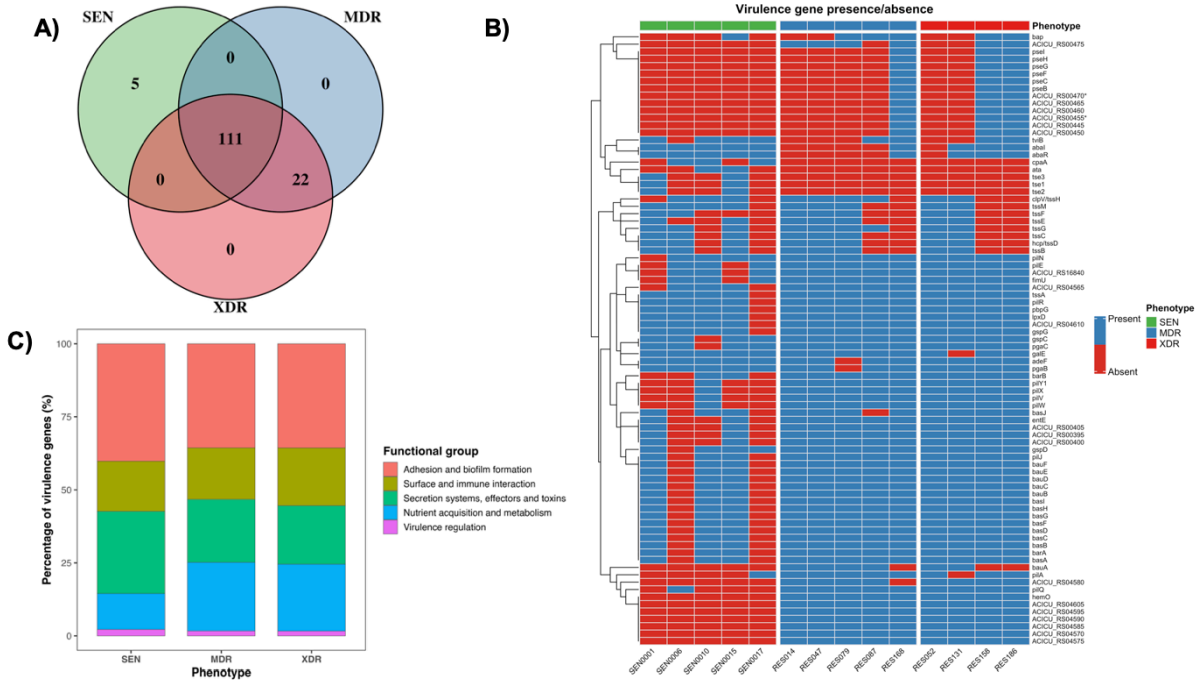

Comparative analysis of virulence-associated genes among susceptible (SEN), multidrug-resistant (MDR), and extensively drug-resistant (XDR) isolates initially identified as *A. baumannii*. (A) Venn diagram showing shared and phenotype-associated virulence genes. (B) Presence/absence heatmap of virulence-associated genes detected by genome-based screening. Blue cells indicate gene presence and red cells indicate gene absence. Hierarchical clustering was based on virulence gene presence/absence profiles. (C) Relative distribution of virulence functional categories across resistance phenotypes, including adhesion and biofilm formation, nutrient acquisition and metabolism, surface and immune interaction, secretion systems/effectors/toxins, and virulence regulation.

Figure 7

See image above for figure legend

Supplementary Files

This is a list of supplementary files associated with this preprint. Click to download.

- SupTablesFinal.pdf